Journal of Geoscience and Environment Protection, 2023, 11, 90-117
https://www.scirp.org/journal/gep
ISSN Online: 2327-4344
ISSN Print: 2327-4336

A Comparative Structural Study of Southern Region Shallow Basement of the North-Kivu Province (DR Congo) by Gravity and Magnetic Data Analysis

Albert Mbata Muliwavyo[1], Jonathan Musitu Muliwavyo[2,3], Lumière Musitu[1], Jean-Marie Joackim Hangi Vuvuya Kataka[1], Jean-Marie Tshitenge Mbuebue[1], Clément N'Zau Umba-Di-Mbudi[2,3,4]

[1]Mention Physics, Faculty of Science and Technology, University of Kinshasa, Kinshasa, Democratic Republic of the Congo
[2]Mention Geosciences, Faculty of Sciences and Technologies, University of Kinshasa, Kinshasa, Democratic Republic of the Congo
[3]Geo-Hydro-Energy Research Group, Faculty of Science and Technology, University of Kinshasa, Kinshasa, Democratic Republic of the Congo
[4]Faculty of Polytechnic, President Joseph Kasa-Vubu State University, Boma, Democratic Republic of the Congo
Email: albert.mbata@unikin.ac.cd, mbaalbert@gmail.com, musitujosephjo@gmail.com, lumieremusitu4@gmail.com, johnmaryhangi@gmail.com, jeanmarie.tshitenge@unikin.ac.cd, Clement.mbudi@unikin.ac.cd

How to cite this paper: Mbata Muliwavyo, A., Musitu Muliwavyo, J., Musitu, L., Hangi Vuvuya Kataka, J.-M. J., Tshitenge Mbuebue, J.-M., & Umba-Di-Mbudi, C. N. (2023). A Comparative Structural Study of Southern Region Shallow Basement of the North-Kivu Province (DR Congo) by Gravity and Magnetic Data Analysis. *Journal of Geoscience and Environment Protection, 11,* 90-117.
https://doi.org/10.4236/gep.2023.119007

Received: July 21, 2023
Accepted: September 12, 2023
Published: September 15, 2023

Abstract

The aim of this study is to characterize the subsoil in the southern region of the North-Kivu province (DR Congo). Gravity and geomagnetic data were used in this study. Five different filters—the horizontal gradient magnitude, the analytic signal, the tilt derivative, the horizontal derivative of tilt derivative and the tilt angle of horizontal gradient—enabled us to delineate the gravity and magnetic anomaly sources present in the shallow subsurface of the study area. The plains of the Rutshuru territory are dominated by sources of weak gravity anomalies and sources of very weak magnetic anomalies located almost in the same places. The southern part of Rutshuru territory and a large part of Masisi territory are underlain by shallow sources of high gravity and magnetic anomalies. Gravity and magnetic anomaly sources are almost identical in the study area. The shallow sources of gravity and magnetic anomalies encountered in our study area are more or less linear and connected. The numerous gravity and magnetic lineaments present in our study region have three major directions: oriented East-West, North-South and North-East-South-West.

Keywords

Gravity, Geomagnetic, Analytic Signal, Tilt Derivative, Horizontal Gradient

1. Introduction

Located in the East of the Democratic Republic of the Congo (DRC), the southern part of the province of North Kivu is endowed with a very rich and varied biodiversity and a subsoil rich in strategic minerals. Among the geophysical methods of prospecting, gravimetry and magnetometry are preliminary methods used in mining exploration and exploitation. These methods make possible a structural mapping of the anomalies' sources of the subsurface and a large coverage of an inaccessible territory without much expense. In a country like the DRC where the geographical, socio-political and infrastructural context does not allow access to certain regions for scientific research, the use of such methods is essential. This context leads us to take an interest in studying the subsoil structure of the southern region of North Kivu, a region that has been and is still the theater of wars for economic purposes.

The exploitation of colombo-tantalite (coltan), cassiterite (tin), wolframite, niobium (pyrochlore), tantalum, tungsten and gold has fueled (Gaudard et al., 2013; Shalaby et al., 2012) and today fuels a violent conflict in this region. To palliate to the lack of field data, we resorted to gravity and geomagnetic fields' data stored in certain databases.

To our knowledge, too little research using the geophysical methods of gravity and magnetic prospecting has been carried out in this study area. However, gravity and magnetic prospecting are preliminary to any prospecting on a given site because it is less expensive than other methods (Hinze et al., 2015). Gravity and geomagnetic field methods are based respectively on the differences in density and magnetic susceptibility of rocks and their distribution in the ground. These methods are used in the exploration and exploitation of natural resources, hydrogeology, civil engineering, archeology, environmental studies, etc. (Launay, 2018).

The location of the vertical borders of the sources of anomalies remains a major concern in the characterization of the subsoil of a given site (Pham, 2020; Askari, 2014).

This paper, therefore, aims to provide information in the geophysical context by relying on gravity and geomagnetic fields in the structural characterization of the subsurface of the southern part of North Kivu.

The southern region of North Kivu is understudied for various reasons (Turnbull et al., 2021). This ignorance of the subsoil structure of this region constitutes an obstacle to the harmonious development of the region in question because the decision-makers cannot make appropriate decisions relating to the rational exploitation of the environment.

The structural mapping of the subsoil of this region is little known to the scientific community. A structural characterization of the subsoil of this region by gravity and magnetic methods could enlighten the scientific community on the structure of the study region subsurface and lead to a rational exploitation of the environment.

2. Description and Geology of the Region

The study area is located in the South-East of North Kivu province in the Democratic Republic of the Congo (DRC) between latitudes 01˚40'00" South and 0˚40'00" South and longitudes 28˚24'00" East and 29˚36'00" East (Figure 1).

The study area belongs to the high mountain region of eastern DRC, with altitudes ranging from 993 m to over 4000 m, and has a deep valley in its north-eastern part (Figure 2).

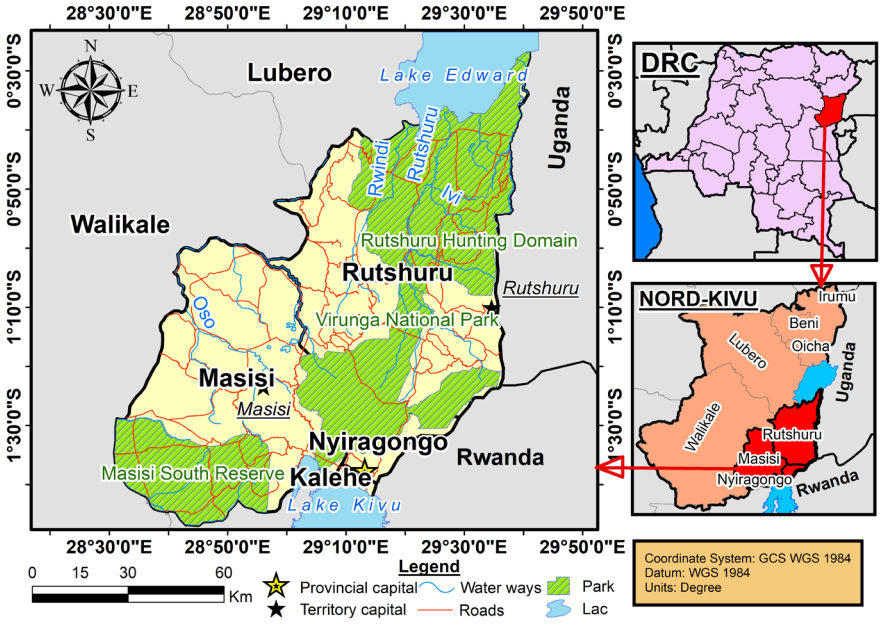

Figure 1. Location map of the study area.

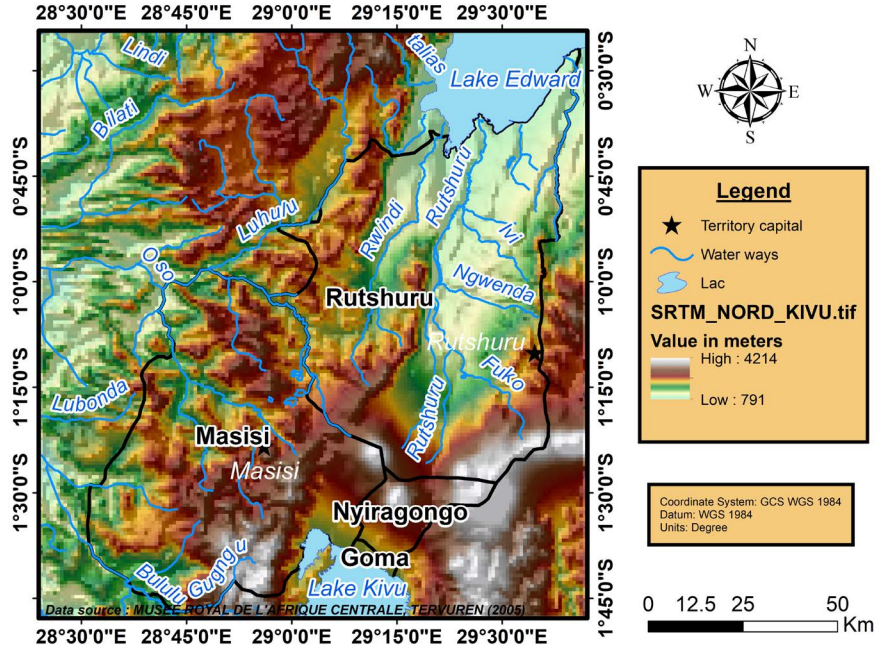

Figure 2. Hydrographical and topographical map of the study region.

The topography of the southern part of North Kivu is made up of plains, plateaux and mountain ranges. The plateaux are located in the South of the region, more specifically in the South-East of the Masisi territory and in the North of the Nyiragongo territory. A plain is located to the South of the Lake Edouard in the Rusthuru territory. This is the Rwindi-Rutshuru plain. To the South, it runs up against the lava fields that relay it towards the Virunga Mountains, more precisely, towards the group of active volcanoes (https://www.congovirtuel.com).

The climate is closely linked to the topography; the study region is characterized by four seasons (https://documents1.worldbank.org): two rainy seasons, the first between mid-August and mid-January and the second practically from mid-February to mid-July; two dry seasons, the first between mid-January and mid-February and the second between mid-July and mid-August.

According to the report by the North Kivu Provincial Planning Ministry (Ministère Provincial du Plan, 2017): below 1000 m altitude the average temperature is close to 23˚C, 19˚C at 1500 m and 15˚C at 2000 m; average rainfall varies between 1000 and 2000 mm. The lowest monthly rainfall is recorded between January and February and between July and August (https://www.congovirtuel.com). The study area is made up of (**Figure 3**):

- Alluvium, eluvium and colluvium resting on the lacustrine series, beaches and low plains of the Lake Edward;
- Granites and associated;
- Ancient basic lavas corresponding to the ancient volcanism of the region;

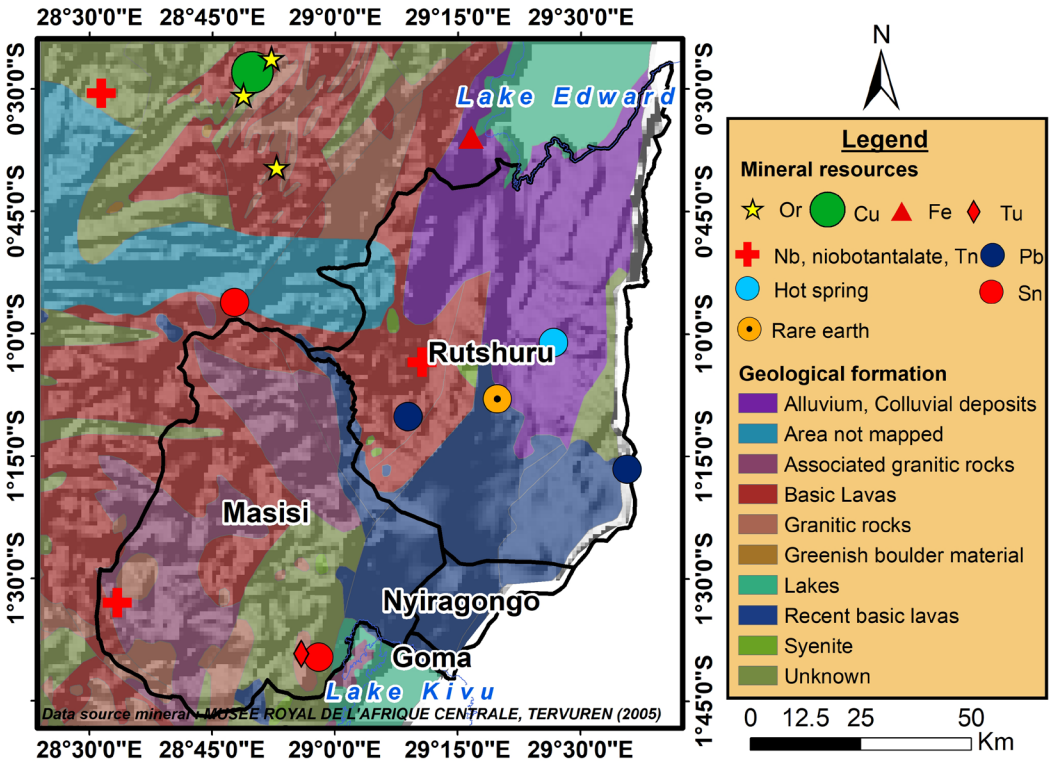

Figure 3. Geological map of our study area.

- Recent basic lavas corresponding to the recent volcanism of the region. Recent volcanism is still ongoing;
- Syenites;
- Pegmatites.

Mineral resources present in our study area are also mapped in Figure 3.

3. Data and Methods

3.1. Data Collection

The complete Bouguer anomalies (CBA)' data of our study region were downloaded from the Bureau International de Gravimétrie (BIG) website (https://bgi.obs-mip.fr). The database is based on 1720 virtual stations equidistant by 3.71 km. The CBA map is shown in Figure 4.

The geomagnetic field intensity data were downloaded on 4 August 2022 from https://ngdc.noaa.gov/geomag/WMM. These data come from satellite and are recorded by the World Magnetic Model (WMM) calculator developed jointly by the National Geophysical Data Center (NGDC) and the British Geological Survey (BGS).

In this work, the 2015 International Geomagnetic Reference Field (IGRF) data is used as the reference for calculating magnetic anomalies. The satellite data concerned by this study are:

- SRTM type for topography (Figure 5);
- Magnetic field intensity data (Figure 6(a));
- IGRF 2015 data incorporated into Oasis montaj 8.4 software (Figure 6(b)).

The difference T - F between the data in Figure 6(a) and those in Figure 6(b) gives a map of the magnetic anomalies (Figure 7).

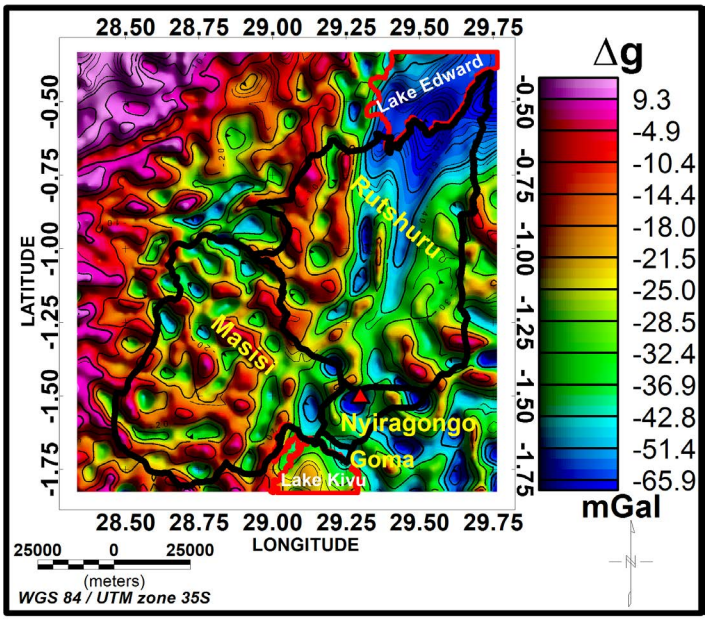

Figure 4. Complete Bouguer anomalies Δg of our study region.

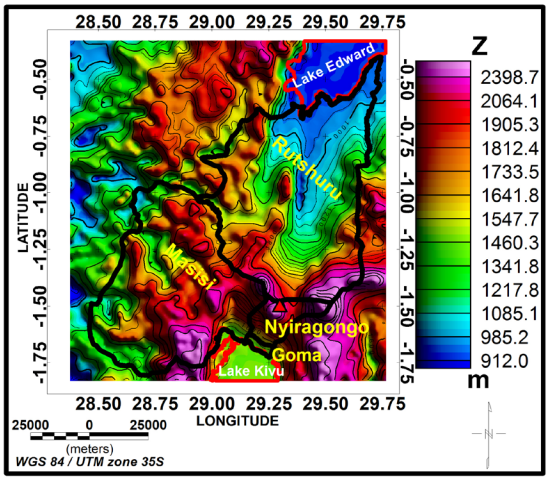

Figure 5. SRTM type for topography of our study area.

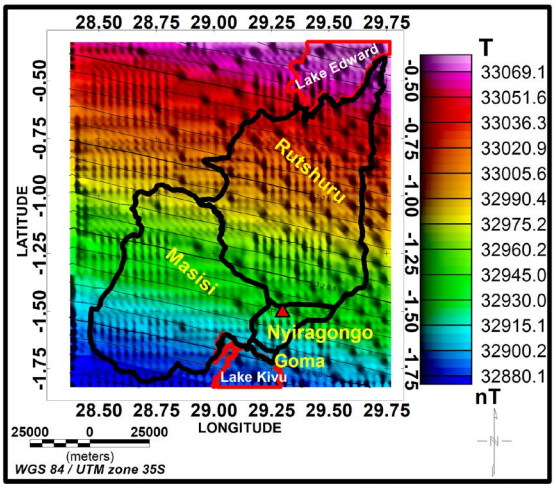

(a)

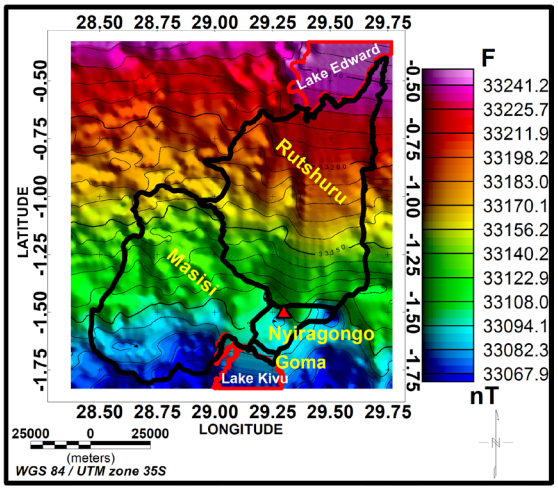

(b)

Figure 6. (a) Earth's magnetic field T in our study region, kriged on 4/8/2022 at an altitude of 3000 m. (b) Regional magnetic field F in our study region, according to the 2015 International Geomagnetic Reference Field.

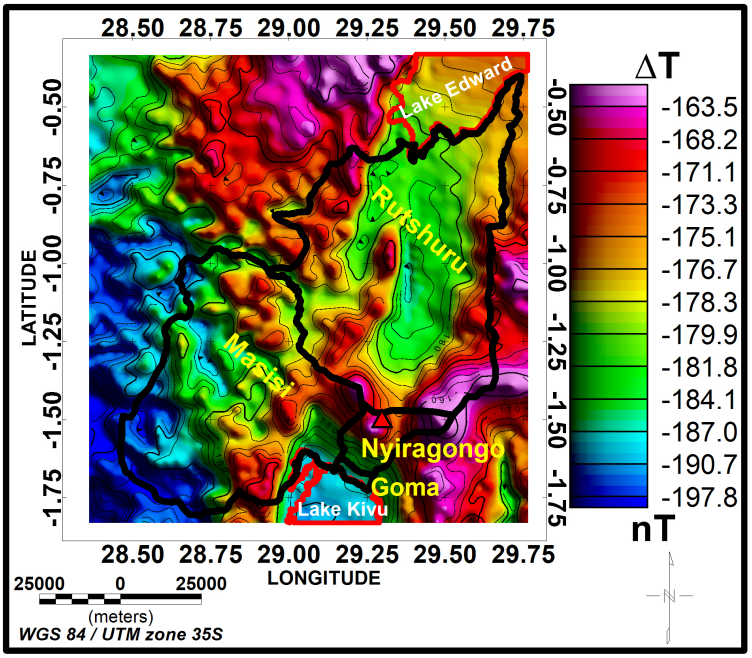

Figure 7. Magnetic anomalies in our study region.

3.2. Data Processing

3.2.1. The Reduction Filter at the Equator

The reduction filter at the equator is a rotation operation that brings the magnetic field back into the horizontal plane. The magnetic anomalies are represented as if they had been measured at the magnetic equator. The reduced to equator magnetic anomalies, ΔB_e, are given by Reynolds (2011):

$$\Delta B_e = \mathcal{F}^{-1}\left\{\psi_e \mathcal{F}\left(\Delta B\right)\right\} \tag{1}$$

with

$$\psi_e = -\left[\frac{\cos(\mu)}{\sin(I)+i\cos(I)\cos(D-\mu)}\right]^2$$

where:

- ψ_e is the filter operator for reduction at the equator in the spectral domain;
- ΔB is the magnetic anomaly of the total field;
- I is the inclination of the Earth's magnetic field;
- D is the declination of the Earth's magnetic field;
- $\mu = \arctan\left(\frac{k_y}{k_x}\right)$;
- k_x and k_y are the components of the wave vector with respect to x and y.

The reduced magnetic anomalies at the equator are shown in Figure 8.

3.2.2. The Upward Continuation Filter

The upward continuation filter transforms the data as if it had been measured at a different height above the source and is defined by Blakely (1995).

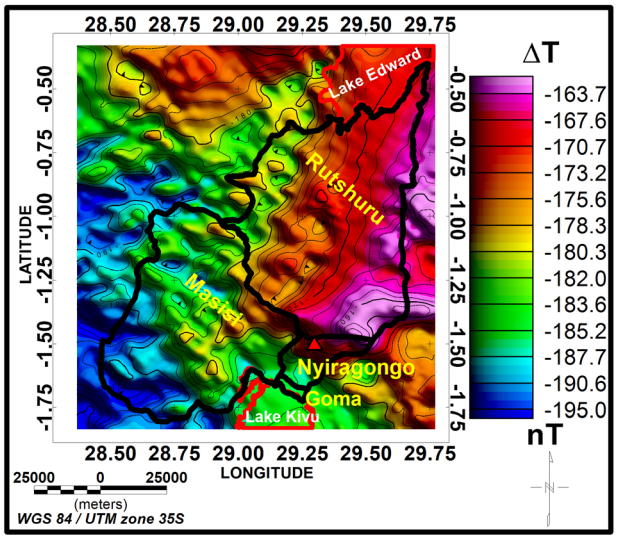

Figure 8. Reduced to equator magnetic anomalies of our study region, $I=-26.51^{\circ}$ and $D=1.22^{\circ}$.

The regional Bouguer and magnetic anomalies, resulting from upward continuation to 500 m elevation, are shown in **Figure 9**.

The residual gravity and magnetic anomalies, obtained after upward continuation at an elevation of 500 m, in our study region are shown in **Figure 10**.

3.3. Methods

Various methods are applied to residual gravity and magnetic anomalies in order to highlight certain characteristics of the shallow subsoil in the southern part of North Kivu. The different methods used in this work are the Horizontal Gradient Magnitude (HGM), the Analytic Signal (SA), the Tilt Derivative (TDR), the horizontal gradient of tilt derivative and the Tilt Angle of Horizontal Gradient (TAHG) magnitude. The various methods used are described in the rest of this work and are implemented, except the TAHG, in the Oasis montaj 8.4 software. All the methods based on the amplitude of gravity and magnetic anomalies display the edges of shallow anomaly sources correctly (Prasad et al., 2022; Pham et al., 2021; Eldosouky et al., 2020; Pham, 2020, 2021). These methods include the horizontal gradient magnitude, the analytic signal and the horizontal derivative of tilt derivative. The legend bar is indicated on some graphs by an abbreviation of the method whose subscript indicates the data type: Δg or ΔB also denoted ΔT.

3.3.1. The Horizontal Gradient

The Horizontal Gradient Magnitude (HGM) is defined by Cordell and Grauch (1985) as:

$$\mathrm{HGM}(x,y)=\sqrt{\left(\frac{\partial \Delta F}{\partial x}\right)^2+\left(\frac{\partial \Delta F}{\partial y}\right)^2} \tag{2}$$

where ΔF is either the gravity anomaly or the magnetic field anomaly.

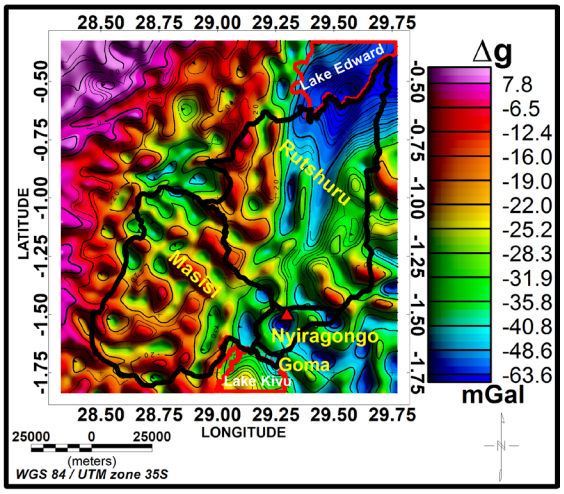

(a)

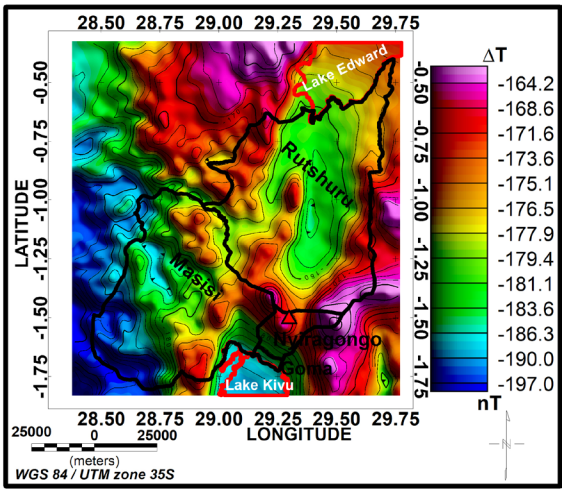

(b)

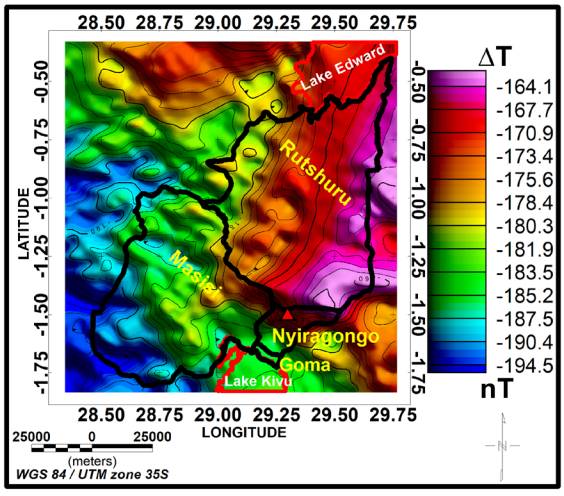

(c)

Figure 9. (a) Regional Bouguer anomalies, (b) regional magnetic anomalies and (c) reduced to equator regional magnetic anomalies obtained after continuation upwards to 500 m elevation.

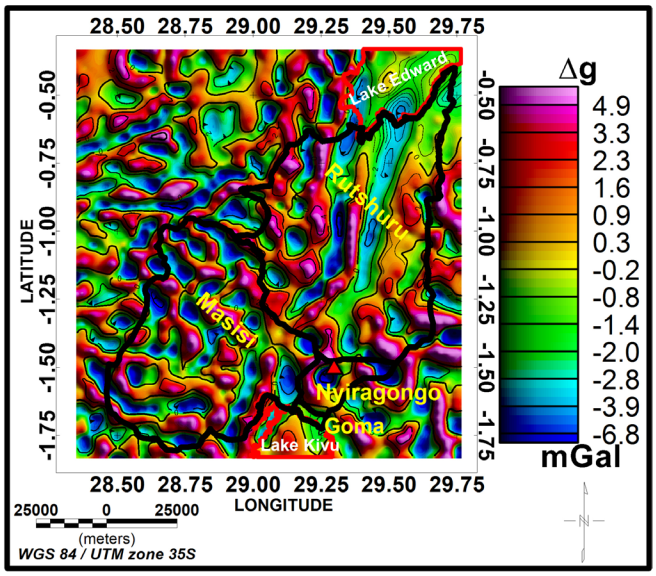

(a)

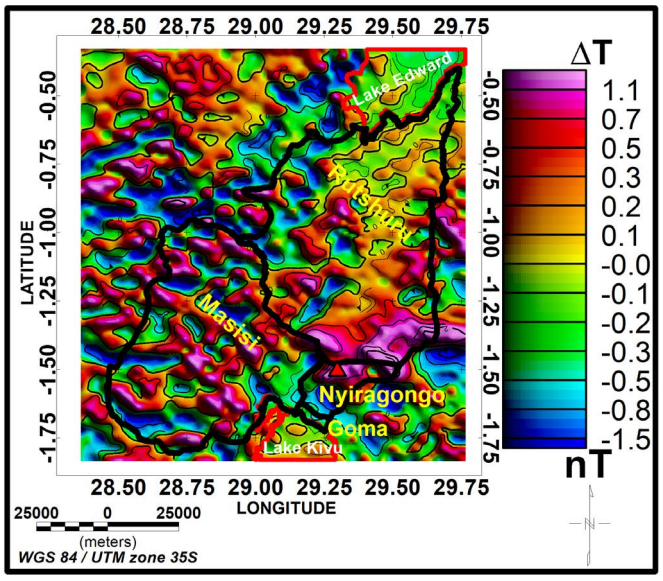

(b)

Figure 10. (a) Residual Bouguer anomalies and (b) reduced to equator residual magnetic anomalies, obtained after upward continuation to 500 m elevation.

The HGM of gravity and magnetic anomalies is used to detect the edges of shallow structures because its maximum values correspond to the horizontal limits of shallow sources (Eldosouky et al., 2020; Pham, 2020, 2021; Pham et al., 2021). The HGM highlights the presence of lineaments and contacts (Pham, 2021).

3.3.2. The Analytic Signal

According to Roest et al. (1992), the Analytic Signal (SA) can be obtained from the derivatives in the three perpendicular directions $\frac{\partial \Delta F}{\partial x}, \frac{\partial \Delta F}{\partial y}$ and $\frac{\partial \Delta F}{\partial z}$:

$$\mathrm{SA}(x,y,z)=\sqrt{\left(\frac{\partial \Delta F}{\partial x}\right)^2+\left(\frac{\partial \Delta F}{\partial y}\right)^2+\left(\frac{\partial \Delta F}{\partial z}\right)^2} \tag{3}$$

Like HGM, SA of gravity or magnetic anomalies highlights the horizontal boundaries of shallow structures. HGM and SA do not have sufficient resolution to properly delineate horizontal boundaries (Pham, 2021).

3.3.3. The Tilt Derivative or the Tilt Angle

Introduced by Miller and Singh (1994) for lineament mapping, the Tilt Derivative (TDR) at a point (x,y) is given by equation:

$$\mathrm{TDR}(x,y)=\tan^{-1}\left[\frac{\dfrac{\partial \Delta F}{\partial z}}{\mathrm{HGM}(x,y)}\right] \tag{4}$$

where $\mathrm{HGM}(x,y)$ is the horizontal gradient magnitude. It is based on the phase produced for equalizing the different amplitudes of gravity and magnetic anomalies (Miller & Singh, 1994). The TDR has a maximum value above shallow anomaly (Miller & Singh, 1994). Zero values of the TDR give the horizontal limits of deep (Prasad et al., 2022) and shallow anomaly sources (Eldosouky et al., 2020; Pham, 2020, 2021; Pham et al., 2021). However, secondary boundaries are observed around the actual edges (Prasad et al., 2022).

3.3.4. The Horizontal Derivative of Tilt Derivative

The Horizontal Derivative of Tilt Derivative (HDTDR) is defined by the equation (Verduzco et al., 2004):

$$\mathrm{HDTDR}(x,y)=\sqrt{\left(\frac{\partial \mathrm{TDR}}{\partial x}\right)^2+\left(\frac{\partial \mathrm{TDR}}{\partial y}\right)^2} \tag{5}$$

The HDTDR uses the maximum values to reinforce the horizontal boundaries of shallow sources (Pham, 2021; Askari, 2014). Nevertheless, secondary boundaries are observed around the actual edges (Prasad et al., 2022; Pham, 2020).

3.3.5. The Tilt Angle of the Horizontal Gradient

Introduced by Ferreira et al. (2013), the tilt derivative of the horizontal derivative (called also Tilt Angle of Horizontal Gradient (TAHG)) is defined as:

$$\mathrm{TAHG}=\tan^{-1}\frac{\dfrac{\partial \mathrm{HGM}}{\partial z}}{\sqrt{\left(\dfrac{\partial \mathrm{HGM}}{\partial x}\right)^2+\left(\dfrac{\partial \mathrm{HGM}}{\partial y}\right)^2}} \tag{6}$$

where

$$\mathrm{HGM}=\sqrt{\left(\frac{\partial \Delta F}{\partial x}\right)^2+\left(\frac{\partial \Delta F}{\partial y}\right)^2}$$

with ΔF the gravity or the magnetic anomaly. The TAHG method can generate a balanced image for the anomaly sources located at different depths (Prasad et al.,

2022) and detect all the source edges without any false edges (Pham et al., 2021).

4. Results and Discussions

4.1. Potential Field Anomalies

4.1.1. Gravity Anomalies

Low Δg values range from −65.9 mGal to −38.7 mGal and are observed in the North-East of the Rutshuru territory, in the North, the South and the West of the Masisi territory, and in the North-East and the Center of the Nyiragongo territory (**Figure 4**). In the West, the Center and the East of the Rutshuru territory, in the Masisi territory and in the west and north of the Nyiragongo territory, intermediate Δg values ranged from −38.7 to −22.7 mGal (**Figure 4**).

The high Δg values range from −22.7 to 9.3 mGal and are found in the West, the Center and the South-East of the Rutshuru territory and in the Masisi territory (**Figure 4**). The gravity anomaly map highlights the following facts (**Figure 4**):

- From East to West of the Rutshuru territory, there are sources of high anomalies which alternate with sources of low anomalies. These anomalies extend from the North to the South of the Rutshuru territory;
- In the Masisi territory, low anomalies' sources are scattered among sources of high anomalies;
- In the Nyiragongo territory, sources of low gravity anomalies are the predominant sources.

4.1.2. Magnetic Field Anomalies

In the East, the North-West and the Center of the Rutshuru territory, in the North and the East of the Masisi territory and in the North of the Nyiragongo territory, the high ΔB values vary between −176.7 and −163.5 nT (**Figure 7**). The higher ΔB values observed in the North of the Nyiragongo territory and in the South-East of the Rutshuru territory could be due to the presence of active and "extinct" volcanoes.

Intermediate values of ΔB range from −187.0 to −176.7 nT and are observed in the West and the Center of the Rutshuru territory, in the North, the Center, the West and the South-East of the Masisi territory and in the South-West of the Nyiragongo territory (**Figure 7**).

In the Center of the Rutshuru territory and in the West and South-West of the Masisi territory, low ΔB values ranged from −187.0 to −197.8 nT (**Figure 7**).

Regional gravity and magnetic anomaly maps show the following facts (**Figure 7**):

- The South-West of the Masisi territory and the West of the Rutshuru territory are characterized by sources of high gravity anomalies or high densities, although there are a few sources of medium gravity anomalies or densities near Earth density in this area;
- In the South of the Rutshuru territory and in the Nyiragongo territory, there are a few medium gravity anomalies scattered among sources of weak gravity

anomalies or densities inferior to Earth density;

- The western and southern parts of the Rutshuru territory and the eastern part of the Masisi territory have sources of high magnetic anomalies or high magnetic susceptibilities and gravity anomalies in their subsurface.

4.2. The Horizontal Gradient of Anomalies or the Amplitude of the Horizontal Gradient

In the East, the South, the West and the Center of the Rutshuru territory high values of $\mathrm{HGM}_{\Delta g}(x,y)$ varying between 356 and 130.4 mGal/m. They are also observed in the West, the North-West and North-East of the Nyiragongo territory and in the Masisi territory as shown in Figure 11.

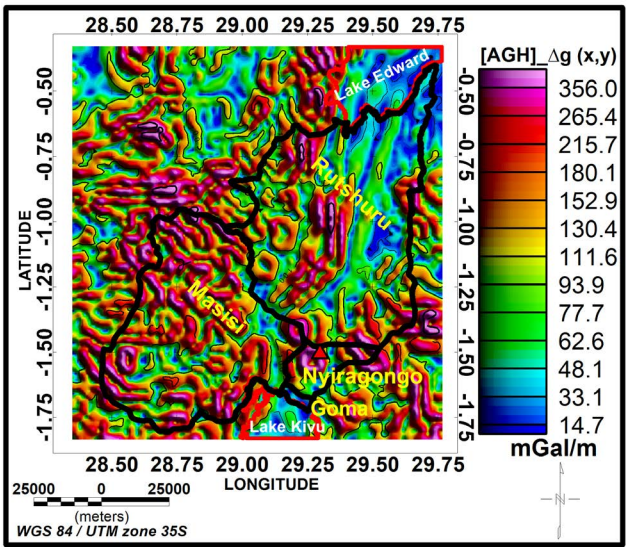

(a)

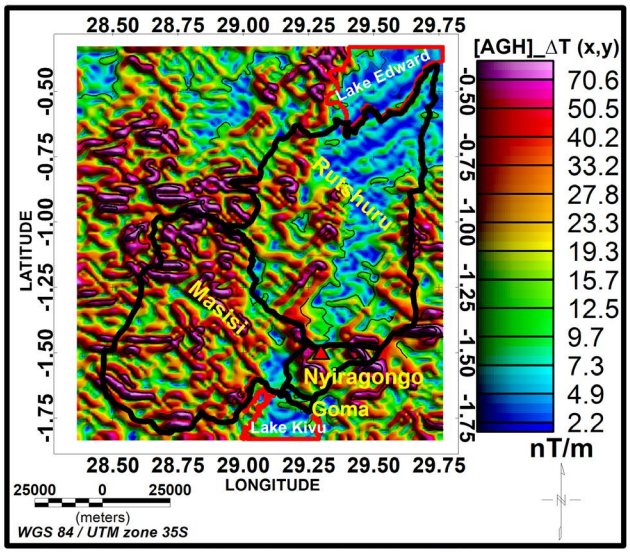

(b)

Figure 11. (a) Horizontal gradient of residual Bouguer anomalies. (b) Horizontal gradient of reduced to equator magnetic anomalies. HGM is denoted in figure as AGH.

The intermediate values of $\mathrm{HGM}_{\Delta g}(x,y)$ range from 111.6 to 62.6 mGal/m and are observed in the South, the North, the Center, the West and the East of the Rutshuru territory, in the South-West and the Center of the Nyiragongo territory and in the Masisi territory.

In the West, the East, the South and the North of the Rutshuru territory, in the South-West and the North of the Nyiragongo territory, in the South and the East of Masisi territory, the low values of $\mathrm{HGM}_{\Delta g}(x,y)$ vary between 48.1 and 14.7 mGal/m.

The low values of $\mathrm{HGM}_{\Delta B}(x,y)$ range from 7.3 to 2.2 nT/m and are observed in the West, South, in the North-East and the Center of the Rutshuru territory, in the South-West and South-East of the Masisi territory.

In the North, the South, the East and the West of the Rutshuru territory, in the West of the Nyiragongo territory and in Masisi territory, the intermediate values of $\mathrm{HGM}_{\Delta B}(x,y)$ vary from 19.3 to 9.7 nT/m.

In the East, the West, the South and the Center of the Rutshuru territory, in the Nyiragongo territory and in the Masisi territory, high values of $\mathrm{HGM}_{\Delta B}(x,y)$ range from 70.6 to 23.3 nT/m.

As the maximum values of $\mathrm{HGM}_{\Delta g}(x,y)$ and $\mathrm{HGM}_{\Delta B}(x,y)$ indicate the edges of shallow structures (**Figure 11**), the study area could contain close geological contacts at the surface.

Some gravity lineaments in our study area are not only more or less parallel to each other but also more or less parallel to the magnetic lineaments, and other gravity lineaments intersect and/or are perpendicular to the magnetic lineaments (**Figure 12**).

Some mineral resources are located in the vicinity sometimes even on the limit of gravity and magnetic lineaments as attested in **Figure 13**.

4.3. The Analytic Signal

In the West, the South, the East and the North-East of the Rutshuru territory, in the Center and South-West of the Nyiragongo territory, and in the East and South of the Masisi territory, the low values of $\mathrm{SA}_{\Delta g}(x,y,z)$ range from 84.6 to 34.0 mGal/m (**Figure 14**).

The intermediate values of $\mathrm{SA}_{\Delta g}(x,y,z)$ vary between 174.2 and 105.9 mGal/m and are observed in the East, the West, the South, the North and the Center of the Rutshuru territory, the South-East and the Center of the Nyiragongo territory, the North, the East, the South and the West of the Masisi territory.

In the South, the East, the West, the North-West and the Center of the Rutshuru territory, in the North-West and the North-East of the Nyiragongo territory and in the Masisi territory, high values of $\mathrm{SA}_{\Delta g}(x,y,z)$ range from 514.6 to 200.1 mGal/m.

The high values of $\mathrm{SA}_{\Delta B}(x,y,z)$ range from 106.3 to 36 nT/m are observed in the West, the East, the South, the Center and the North-West of the Rutshuru territory and in the Nyiragongo territory and the Masisi territory.

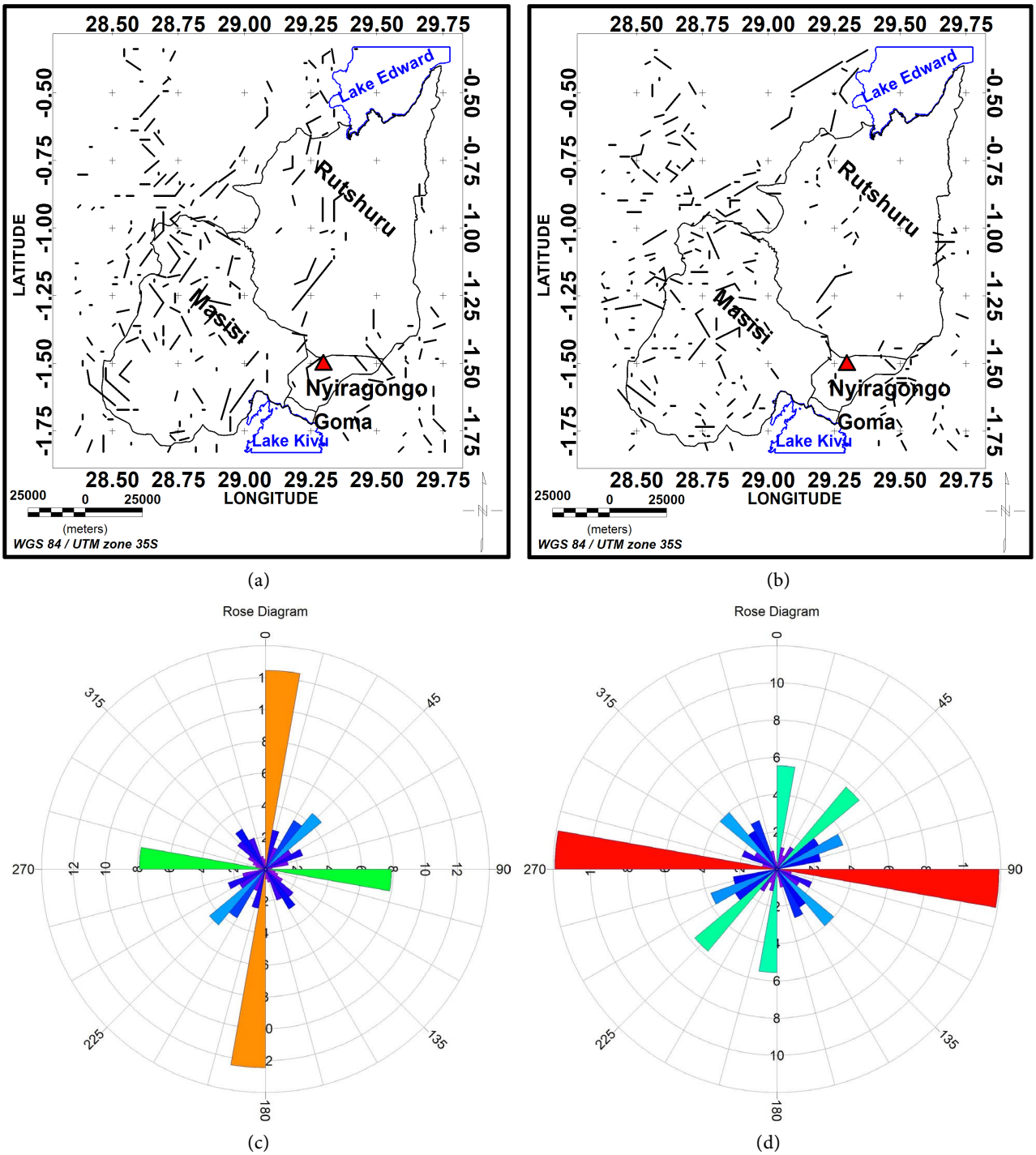

Figure 12. (a) Lineaments derived from the horizontal gradient of residual Bouguer anomalies. (b) Reduced to equator residual magnetic anomalies. (c) Rose diagram of residual Bouguer anomalies. (d) Rose diagram of reduced to equator magnetic anomalies.

Intermediate values of magnetic anomalies' SA range from 30.6 to 15.8 nT/m and are observed in the West, the South, the North and the East of the Rutshuru territory, in the South-West and the West of the Nyiragongo territory and in the Masisi territory.

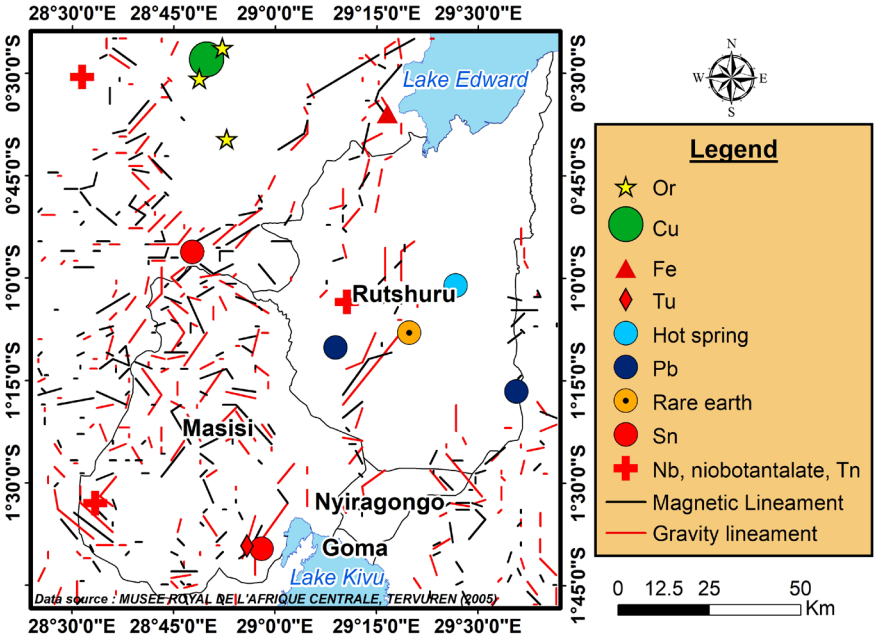

Figure 13. Map of mineral resource indices superimposed on lineaments' map arising from HGM.

In the West, the North and the East of the Rutshuru territory, in the North-West of the Nyiragongo territory, in the East, the South-West and the North of the Masisi territory, the low values of magnetic anomalies' SA range from 11.9 to 4.5 nT/m.

The maximum values of gravity anomalies' SA and magnetic anomalies' SA indicate the edges of shallow structures (Figure 14). Figure 14(a) and Figure 14(b) have some similarities. The high values of gravity anomalies' SA and magnetic anomalies' SA could characterize shallow rocks with high variation in density or magnetic susceptibility. Low amplitude anomaly sources are difficult to recognize among higher amplitude anomaly sources when using HGM, SA and their enhanced versions (Eldosouky et al., 2022). Moreover, Prasad et al. (2022) note that the HGM and AS filters cannot delineate deeper bodies and anomalies' amplitudes from the sources located at different depths.

HGM and SA applied to gravity and magnetic anomalies in our study region show that:

- The eastern part of the Rutshuru territory has shallow underground sources of anomalies with almost the same boundaries. In this case, the sources of gravity anomalies and the sources of magnetic anomalies are almost the same in the study area;
- The plains of the Rutshuru territory are dominated by sources of weak gravity anomalies and sources of weak magnetic anomalies;
- The southern part of the Rutshuru territory and a large part of the Masisi territory have subsoil sources of high gravity and magnetic anomalies. Magnetic sources with medium anomalies are sparse in this region;

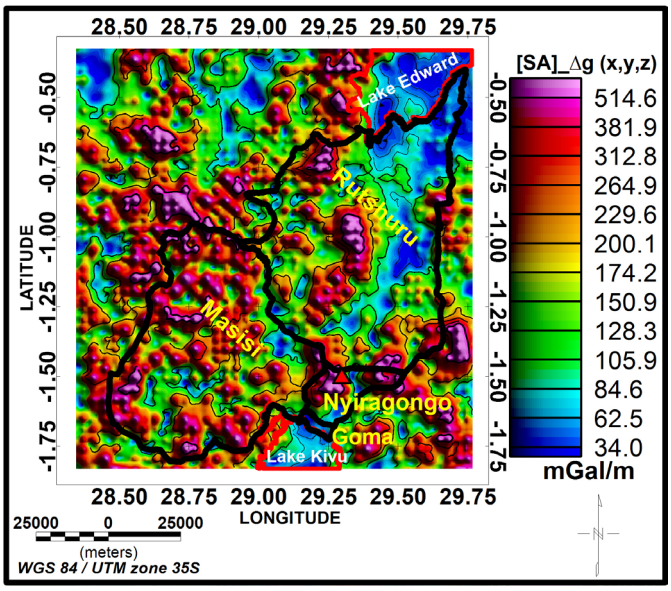

(a)

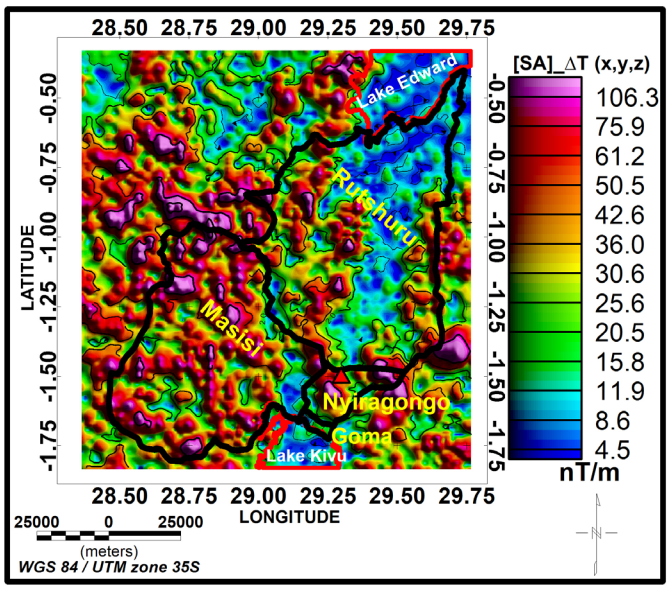

(b)

Figure 14. (a) Analytic signal of residual Bouguer anomalies. (b) Analytic signal of reduced to equator magnetic anomalies.

- The northern part of the Nyiragongo territory is dominated by structures with high HGM or SA values.

The gravity and magnetic lineaments would have two structural directions: N-S, NE-SW and W-E (Figure 15). Some mineralizations are near the gravity and magnetic lineaments (Figure 16).

4.4. The Tilt Derivative

The directional derivative applied to the residual gravity and magnetic anomalies is shown in Figure 17.

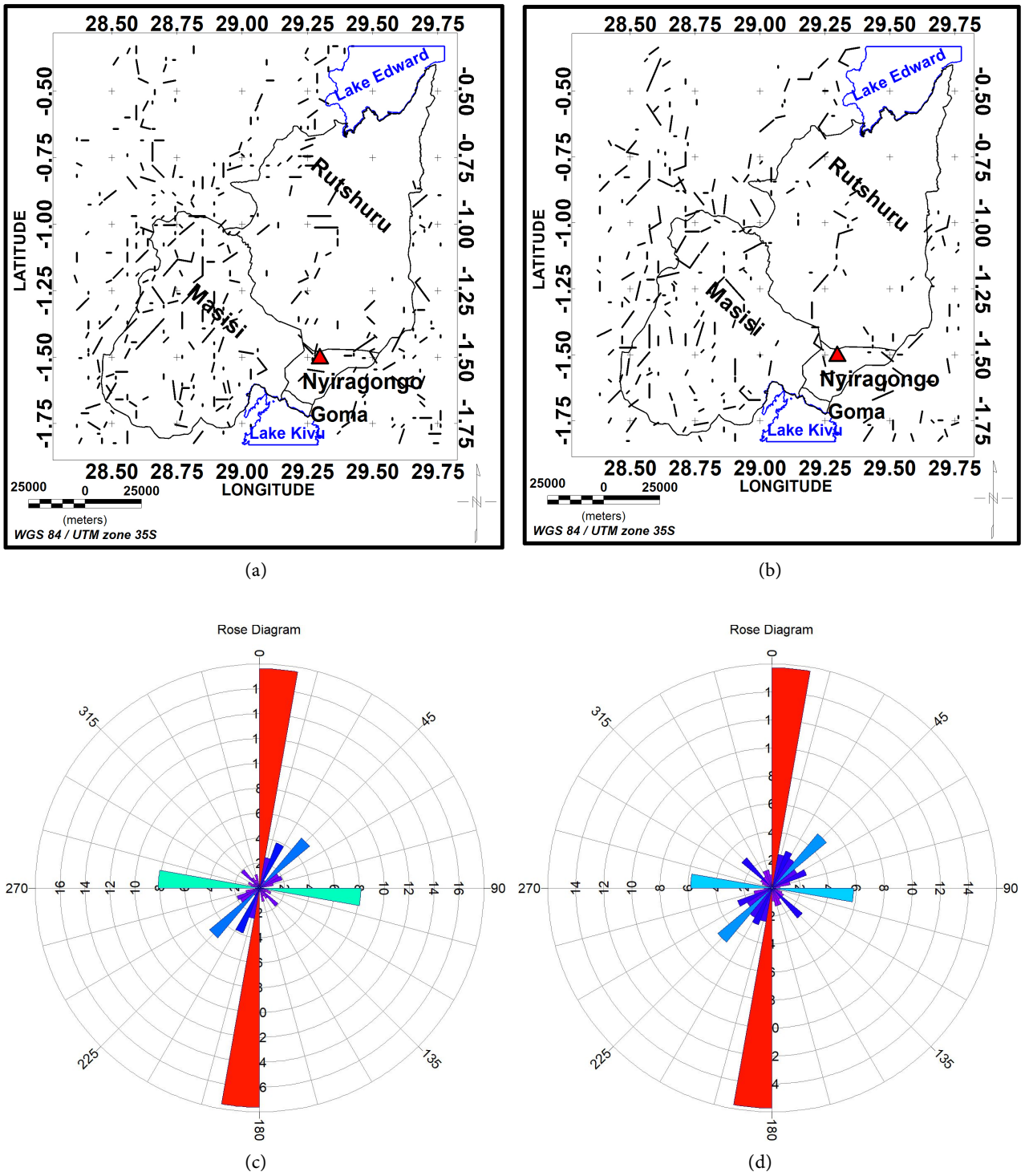

Figure 15. (a) Lineaments derived from AS of residual Bouguer anomalies. (b) Lineaments derived from AS of residual reduced to equator magnetic anomalies. (c) Rose diagram of the lineaments derived from AS of residual Bouguer anomalies. (d) Rose diagram derived from AS of reduced to equator magnetic anomalies.

The high values of $\mathrm{TDR}_{\Delta g}(x, y)$, ranging from 0.4 to 1.25 radians, are observed in the West, the Center, the North and South-West of the Nyiragongo territory and in the Masisi territory and the Rutshuru territory.

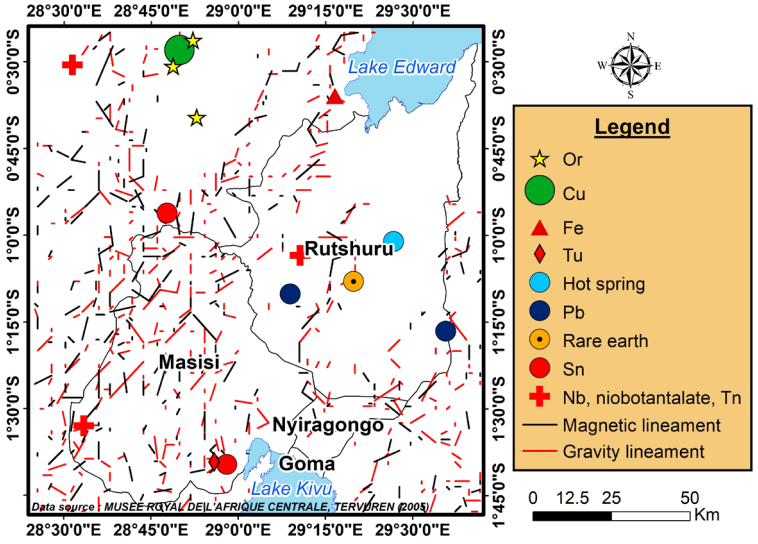

Figure 16. Map of mineral resource indices superimposed on lineaments' map arising from AS.

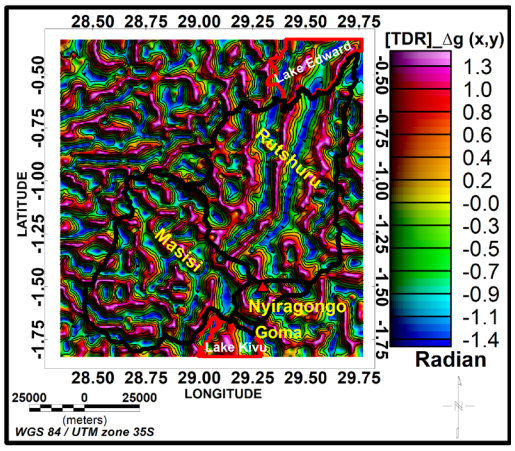

(a)

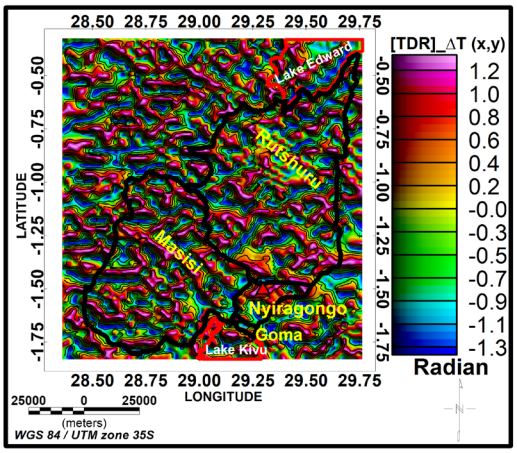

(b)

Figure 17. (a) Tilt derivative of residual Bouguer anomalies. (b) Tilt derivative of reduced to equator residual magnetic anomalies.

The TDR higher values of magnetic anomalies vary between 0.2 and 1.2 radians and are observed in the North and the East of the Nyiragongo territory, in the East, the West, the South and the Center of the Rutshuru territory and in the Masisi territory. Negative values of gravity anomalies' TDR in the Rutshuru territory can be assigned to structures of low density. Taking into account the geology of the territory of the Rutshuru where there are sedimentary formations of the alluvium, elluvium and colluvium type, it is likely that the negative values of TDR and even the low gravity anomalies are due to the presence of hydrocarbons. As the zero value of the tilt angle of anomalies gives the limits of an anomaly source, negative TDR values of magnetic anomalies are characteristic of non-magnetic rocks and range in our study area from −0.3 to −1.3 radians. The TDR has a maximum value above shallow anomaly. The sources of shallow anomalies revealed by TDR in our study area are more or less linear. As TDR can bring false boundaries in the edge maps (Pham et al., 2021), all the bodies delineated by this filter in our study area should also be considered with care.

The gravity or magnetic lineaments in our study area would have two structural directions: N-S and W-E (**Figure 18**).

Some gravity lineaments are more or less parallel to the magnetic lineaments, and other gravity lineaments intersect and/or are perpendicular to the magnetic lineaments (**Figure 19**). Some indices of mineral resources in our study area are located near or even on magnetic lineaments for this vast region, others near or even on the gravity lineaments (**Figure 19**).

4.5. The Horizontal Derivative of Tilt Derivative

The horizontal derivative of the tilt derivative applied to the residual gravity and magnetic anomalies is shown in **Figure 20**. In the East, the South, the West, the North-East, the North-West and the Center of the Rutshuru territory, in the Nyiragongo territory and in the Masisi territory, the high values of gravity anomalies' HDTDR range from 52.9 to 87.0 radian/m. The higher values of magnetic anomalies'HDTDR, varying between 61.8 and 108.5 radian/m, are observed in the Center, the West and the North-East of the Nyiragongo territory, in the West, the South, the East and the Center of the Rutshuru territory and in the Masisi territory.

The edges of shallow structures revealed in our study area by the maximum gravity and magnetic HDTDR values are more or less linear and interconnected (**Figure 20**). Arisoy and Dikmen (2013) noted that THTDR filter amplifies noise and is not effective in delineating deeper anomaly sources. Thus, all bodies delineated by this filter cannot be considered as real sources; some bodies can be artifacts. In our study area, gravity or magnetic lineaments derived from HDTDR analysis have two structural directions: N-S and W-E as shown in **Figure 21**.

The TDR and HDTDR show differences in the limitation of the edges of the anomaly sources in the three territories of the study area. But certain facts stand out: a large part of the Rutshuru territory is dominated by non-magnetic anomaly sources. This is not the case in the Masisi territory. In addition, the shallow

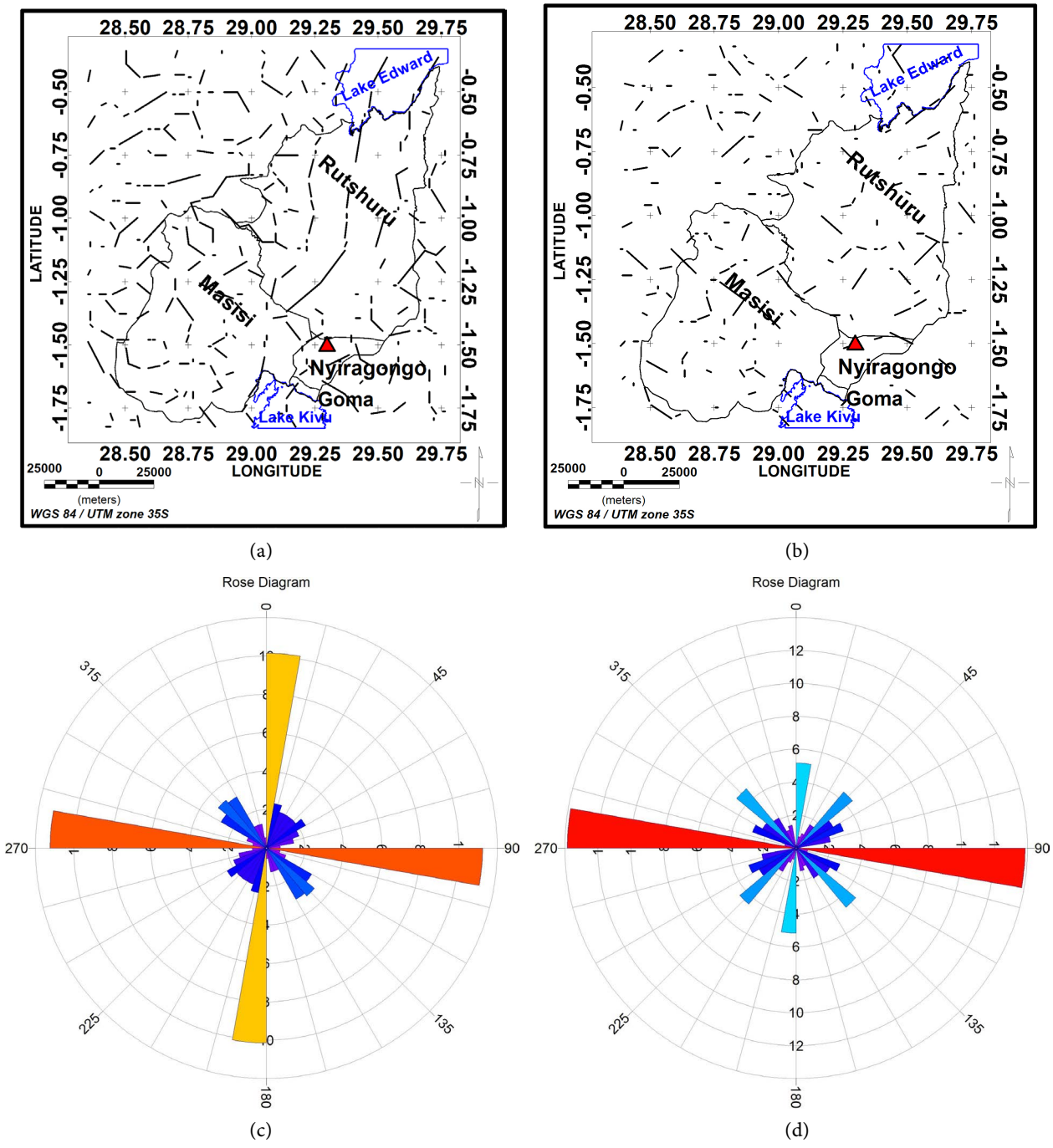

Figure 18. (a) Lineaments derived from the tilt derivative of residual Bouguer anomalies. (b) Lineaments derived from the tilt derivative of residual reduced to equator residual magnetic anomalies. (c) Rose diagram of the lineaments derived from the tilt derivative of residual Bouguer anomalies. (d) Rose diagram of the lineaments derived from the tilt derivative of reduced to equator magnetic anomalies.

anomaly sources in our study area, revealed by TDR and HDTDR, appear to be linear and interconnected, as shown in Figure 17 and Figure 20.

Some gravity lineaments are more or less parallel to that of the magnetic lineaments, and other gravity lineaments intersect and/or are perpendicular to the magnetic lineaments (see Figure 22).

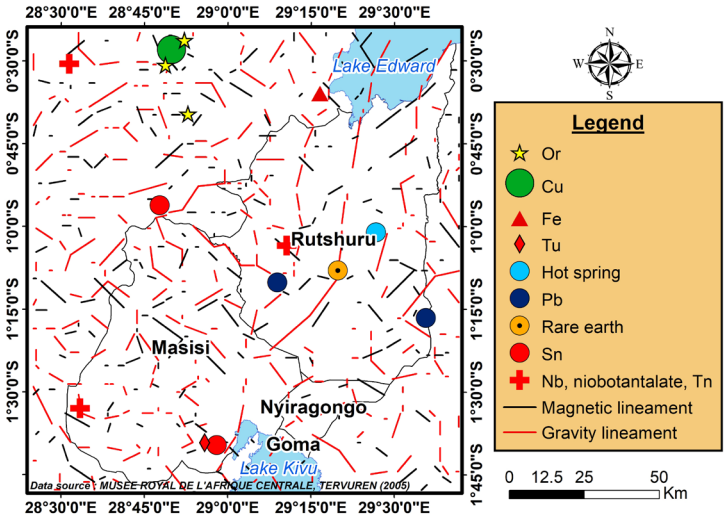

Figure 19. Map of mineral resource indices superimposed on lineaments' map resulting from the tilt derivative.

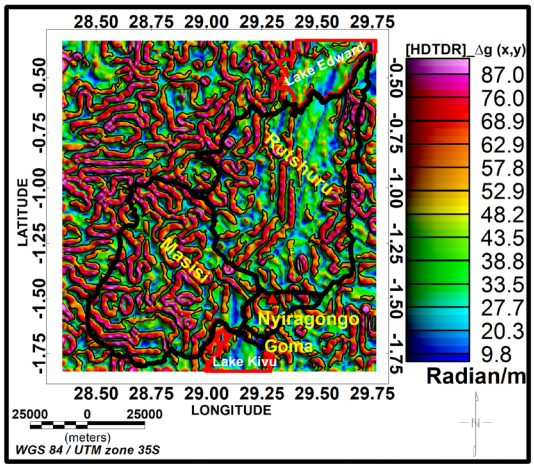

(a)

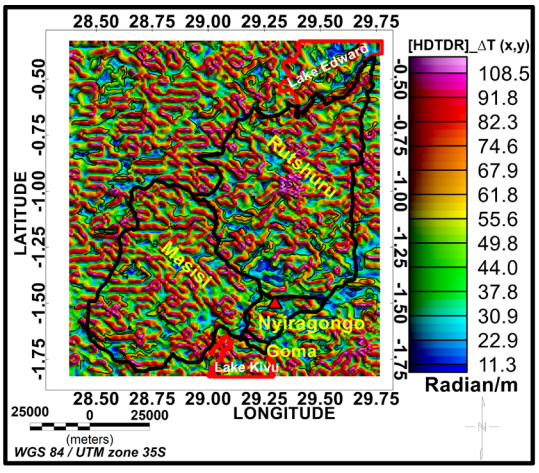

(b)

Figure 20. (a) Horizontal derivative of tilt derivative of residual Bouguer anomalies. (b) Horizontal derivative of tilt derivative of reduced to equator residual magnetic anomalies.

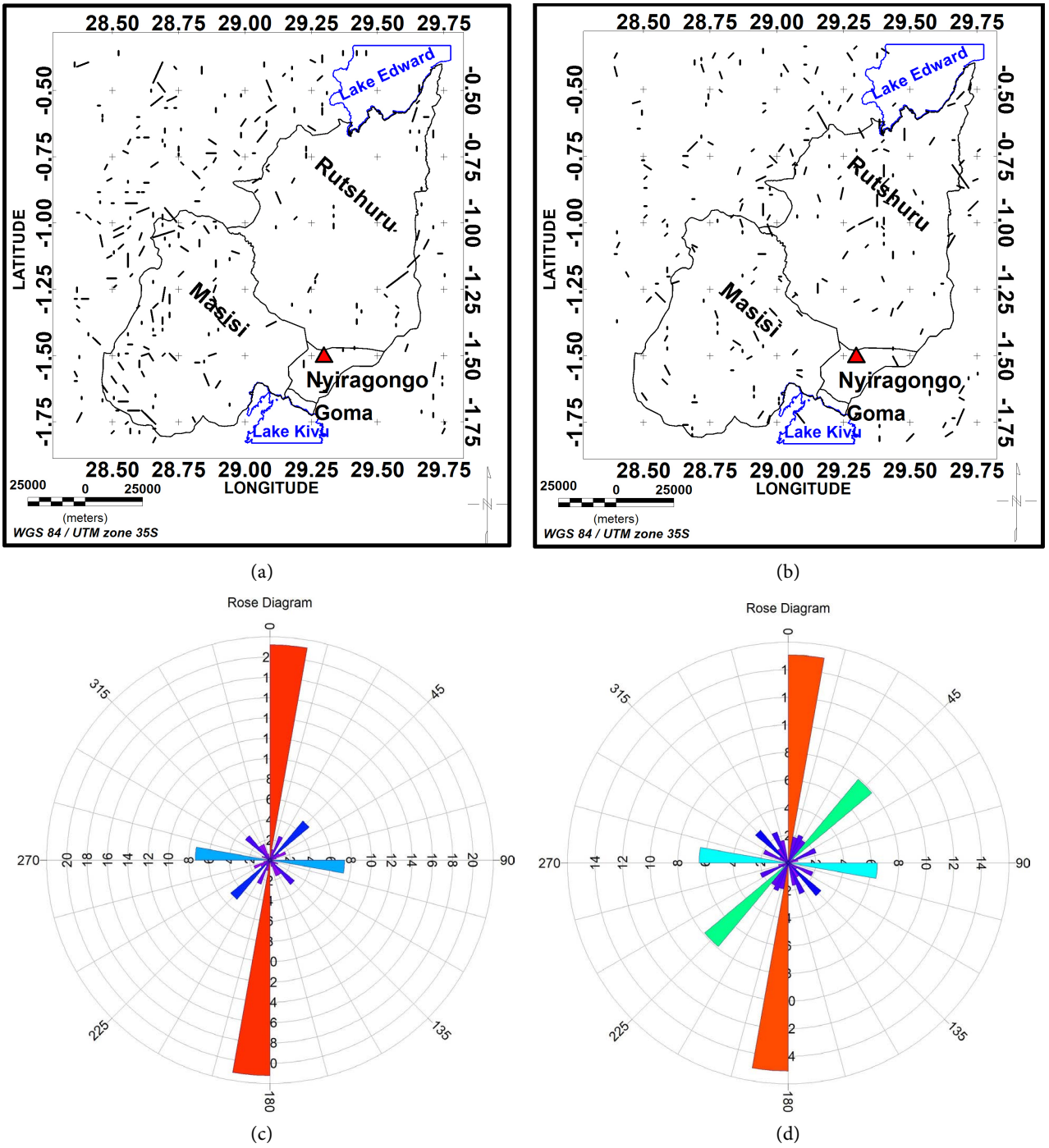

Figure 21. (a) Lineaments derived from the horizontal derivative of tilt derivative of residual anomalies. (b) Lineaments derived from the horizontal derivative of tilt derivative of reduced to equator residual magnetic anomalies. (c) Rose diagram of lineaments derived from the horizontal derivative of tilt derivative of residual Bouguer anomalies. (d) Rose diagram of lineaments derived from the horizontal derivative of tilt derivative of reduced to equator magnetic anomalies.

Some indices of mineral resources in our study area are located near or even on magnetic lineaments, others near or even on the gravity lineaments. In last other indices of mineral resources are not located on one or more lineaments, i.e. no gravity lineaments and no magnetic lineaments as indicated in Figure 22.

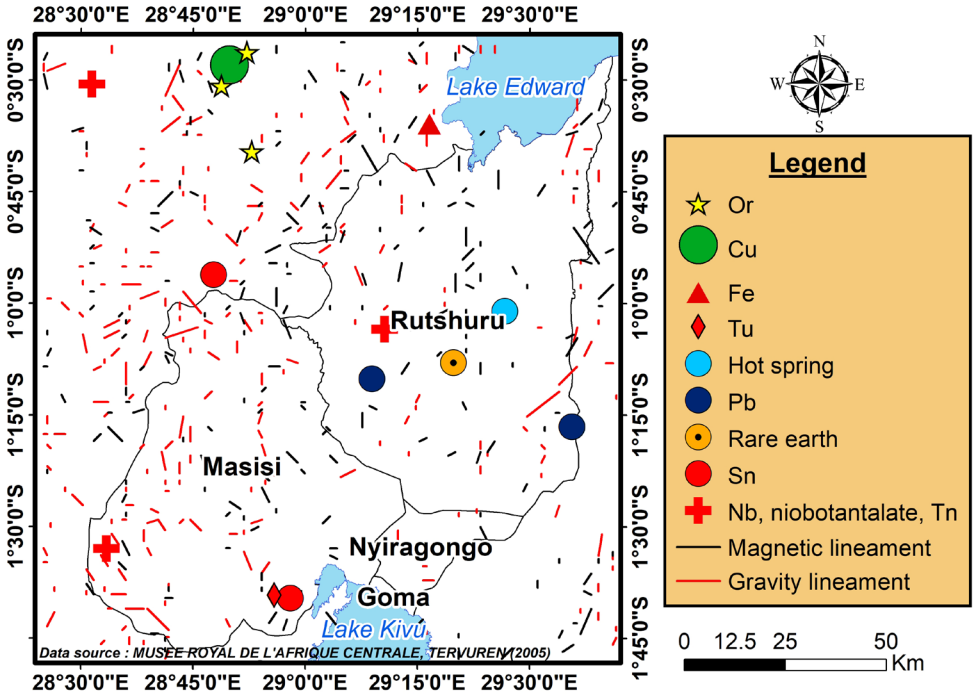

Figure 22. Map of mineral resource indices superimposed on lineaments' map resulting from the horizontal derivative of tilt derivative.

4.6. The Tilt Angle of the Horizontal Gradient

High gravity TAHG values shown in **Figure 23** vary between 0.1 and 1.2 radians and can be linked to geological bodies of high density while positive magnetic TAHG values, varying between 0.0 and 1.2 radians, can reveal rocks of high magnetic susceptibilities.

The negative gravity TAHG values or the negative magnetic TAHG values, ranging from −0.1 to −1.4 radians, are probably linked to deeper bodies or to low density geological bodies and low magnetic susceptibility sources, respectively.

Anomaly sources are almost linear and interconnected in our study area as shown in **Figure 23**. According to Pham et al. (2021), TAHG filter can equalize the large and small amplitude anomalies from sources located at different edges without any false edges. Therefore, it can delineate all the borders of anomaly sources in our study area. However, in presence of anomaly sources of superimposed magnetic structures, it cannot perform well (Prasad et al., 2022) and thus edges of anomaly sources revealed in our study area by TAHG should also be taken with care. Our results from this filter can, therefore, retain our attention and can be compared to those obtained by applying the preceding filters.

Figure 24 presents a synthetic map of study area lineaments derived from results of different filters that have been applied to gravity and magnetic anomalies. The study area would be strewn by several fractures and or lithological contacts as shown in **Figure 24**. This is due to the fact that the study area is located on the western branch of Eastern African Rift.

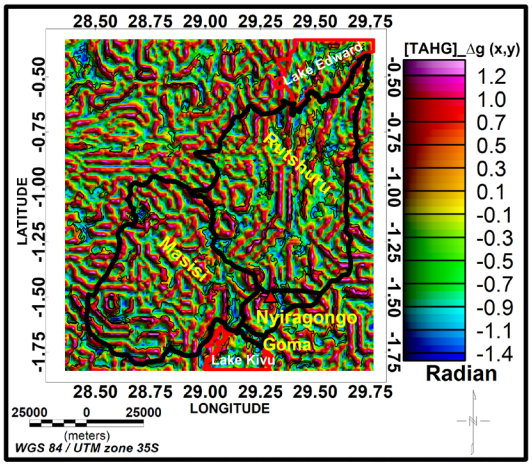

(a)

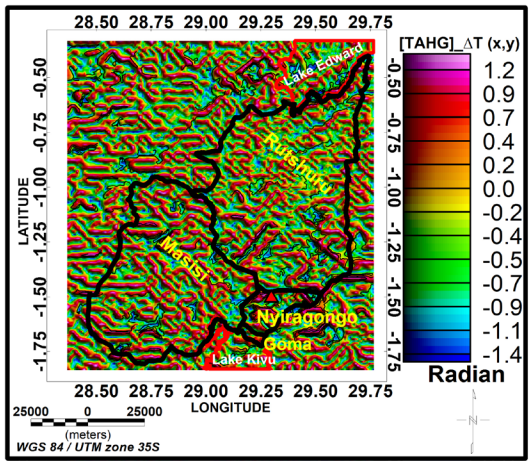

(b)

Figure 23. (a) Tilt angle of the horizontal gradient of residual Bouguer anomalies. (b) Tilt angle of the horizontal gradient of reduced to equator residual magnetic anomalies.

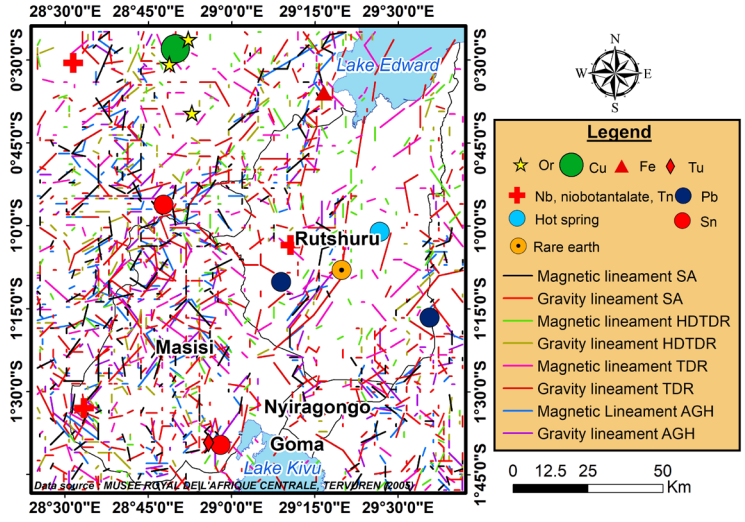

Figure 24. Map of gravity and magnetic lineaments derived from results of all filters, except the TAHG filter, used in this paper.

5. Conclusion

The South-West of the Masisi territory and the West of the Rutshuru territory are characterized by sources of high gravity anomalies, however, in this area, some sources of medium gravity anomalies are found there. The West and South of the Rutshuru territory and the eastern part of Masisi territory have sources of high magnetic anomalies in their subsoil. In the South of the Rutshuru territory and the North of the Nyiragongo territory, there are some medium gravity anomalies' sources scattered among the sources of weak gravity anomalies. The East of the Rutshuru territory presents in its shallow basement sources of gravity and magnetic anomalies having almost the same limits. The sources of gravity anomalies and the sources of magnetic anomalies are almost identical in the study area. The plains of the Rutshuru territory are dominated by sources of weak gravity anomalies and sources of very weak magnetic anomalies. The South of the Rutshuru territory and a large part of the Masisi territory have sources of both gravimetric and high magnetic anomalies that practically coincide. The sources of shallow gravity and magnetic anomalies encountered in our study area are more or less linear and connected. All gravity and magnetic lineaments in our study region have three major directions: East-West, North-South and North-East-South-West. Our work is limited to the characterization of the shallow subsoil of the southern region of the North-Kivu province. The characterization of the deep subsurface may be the subject of further work.

Conflicts of Interest

The authors declare no conflicts of interest regarding the publication of this paper.

References

Arisoy, M., & Dikmen, Ü. (2013). Edge Detection of Magnetic Sources Using Enhanced Total Horizontal Derivative of the Tilt Angle. *Bulletin of the Earth Sciences Application and Research Centre of Hacettepe University, 34,* 73-82.

Askari, A. (2014). Edge Detection of Gravity Anomaly Sources via the Tilt Angle, Total Horizontal Derivative, Total Horizontal Derivative of the Tilt Angle and New Normalized Total Horizontal Derivative. *Scholars Journal of Engineering and Technology, 2,* 842-846.

Blakely, R. (1995). *Potential Theory in Gravity and Magnetic Applications*. Cambridge University Press. https://doi.org/10.1017/CBO9780511549816

Cordell, L., & Grauch, V. (1985). Mapping Basement Magnetization Zones from Aeromagnetic Data in the San Juan Basin, New Mexico. In *The Utility of Regional Gravity and Magnetic Anomaly Maps* (pp. 181-197). Society of Exploration Geophysicists. https://doi.org/10.1190/1.0931830346.ch16

Eldosouky, A. M., Pham, L. T., Abdelrahman, K., Fnais, M. S., & Gomez-Ortiz, D. (2022). Mapping Structural Features of the Wadi Umm Dulfah Area Using Aeromagnetic Data. *Journal of King Saud University—Science 34,* Article ID: 101803. https://doi.org/10.1016/j.jksus.2021.101803

Eldosouky, A., Thanh Pham, L., Mohmed, H., & Pradhan, B. (2020). A Comparative Study of THG, AS, TA, Theta, TDX and LTHG Techniques for Improving Source Boundaries Detection of Magnetic Data Using Synthetic Models: A Case Study from G. Um Monqul, North Eastern Desert, Egypt. *Journal of African Earth Sciences, 170,* Article ID: 103940. https://doi.org/10.1016/j.jafrearsci.2020.103940

Ferreira, F. J. F., de Souza, J., Bongiolo, A. de B. e S., & de Castro, L. G. (2013). Enhancement of the Total Horizontal Gradient of Magnetic Anomalies Using the Tilt Angle. *Geophysics, 78,* J33-J41. https://doi.org/10.1190/geo2011-0441.1

Gaudard, C., Dupre, M., Jorand, J., Mamdy, B., & Ciarabeli, L. (2013). *Pétrole à Muanda: La justice au rabais*. CCFD-Terre Solidaire.

Hinze, J., Von Frese, R., & Saad, H. (2015). *Applications of Gravity and Magnetic Methods to Subsurface Exploration*. Cambridge University Press.

Launay, N. (2018). *Propriétés d'aimantation des sources géologiques des anomalies du champ magnétique terrestre: Magnétisme des roches et modélisation numérique* (pp. 1-228). Ph.D. Thesis, Aix-Marseille Université.

Miller, H., & Singh, V. (1994). Potential Field Tilt—A New Concept for Location of Potential Field Sources. *Journal of Applied Geophysics, 32,* 213-217. https://doi.org/10.1016/0926-9851(94)90022-1

Ministère Provincial du Plan (2017). *Localisation des Objectifs de développement durable dans le Nord-Kivu*. https://knowledge-uclga.org/IMG/pdf/localisationdesodddanslenordkivu.pdf

Pham, L. T. (2020). A Comparative Study on Different Filters for Enhancing Potential Field Source Boundaries: Synthetic Examples and a Case Study from the Song Hong Trough (Vietnam). *Arabian Journal of Geosciences, 13*, Article No. 723. https://doi.org/10.1007/s12517-020-05737-5

Pham, L. T. (2021). A High Resolution Edge Detector for Interpreting Potential Field Data: A Case Study from the Witwatersrand Basin, South Africa. *Journal of African Earth Sciences, 178,* Article ID: 104190. https://doi.org/10.1016/j.jafrearsci.2021.104190

Pham, L. T., Vu, M. D., & Le, S. T. (2021). Performance Evaluation of Amplitude- and Phase-Based Methods for Estimating Edges of Potential Field Sources. *Iranian Journal of Science and Technology, Transaction A: Science, 45,* 1327-1339. https://doi.org/10.1007/s40995-021-01122-3

Prasad, K., Pham, L., Singh, A., Eldosouky, A., Abdelrahman, K., Fnais, M., & Gómez-Ortiz, D. (2022). A Novel Enhanced Total Gradient (ETG) for Interpretation of Magnetic Data. *Minerals, 12,* Article 1468. https://doi.org/10.3390/min12111468

Reynolds, J. (2011). *An Introduction to Applied and Environnemental Geophysics* (2nd ed.). John Wiley & Sons, Ltd.

Roest, W., Verhoef, J., & Pilkington, M. (1992). Magnetic Interpretation Using 3-D Analytic Signal. *Geophysics, 57,* 116-125. https://doi.org/10.1190/1.1443174

Shalaby, H., Bangui, C., Monfort, A., Huart, J., & Bal, J. (2012). *Evaluation Environnementale Stratégique de l'exploration/exploitation pétrolière dans le nord du Rift Albertin (Provinces du Nord-Kivu et de l'Orientale)*. Ministère de l'Environnement, Conservation de la Nature et Tourisme et Ministère délégué chargé des Finances (Ordonnateur national du Fonds Européen de Développement, FED), République Démocratique du Congo.

Turnbull, R., Allibone, A., Matheys, F., Fanning, C., Kasereka, E., Kabete, J. et al. (2021). Geology and Geochronology of the Archean Plutonic Rocks in the Northeast Democratic Republic of Congo. *Precambrien Research, 358,* Article ID: 106133.

https://doi.org/10.1016/j.precamres.2021.106133

Verduzco, B., Fairhead, J., Green, C., & Mackenzie, C. (2004). New Insights into Magnetic Derivatives for Structural Mapping. *The Leading Edge, 23,* 116-119. https://doi.org/10.1190/1.1651454